Surface differential rotation and photospheric magnetic field of the young solar-type star HD 171488 (V889 Her)

S. C. Marsden, J.-F. Donati, M. Semel, P. Petit, B. D. Carter

Mon. Not. R. Astron. Soc. **370,** 468–476 (2006) doi:10.1111/j.1365-2966.2006.10503.x

Surface differential rotation and photospheric magnetic field of the young solar-type star HD 171488 (V889 Her)

S. C. Marsden,[1⋆] J.-F. Donati,[2⋆] M. Semel,[3⋆] P. Petit[2⋆] and B. D. Carter[4⋆]

[1]*Institute of Astronomy, ETH Zurich, 8092 Zurich, Switzerland*
[2]*Laboratoire d'Astrophysique, Observatoire Midi-Pyrénées, F-31400 Toulouse, France*
[3]*LESIA, Observatoire de Paris-Meudon, F-92195 Meudon Cedex, France*
[4]*Faculty of Sciences, University of Southern Queensland, Toowoomba 4350, Australia*

Accepted 2006 April 26. Received 2006 April 25; in original form 2005 September 5

ABSTRACT

We present spectropolarimetric observations of the young, single early G-dwarf HD 171488. These observations were obtained over a five-night period in 2004 September at the 3.9-m Anglo-Australian Telescope using the SEMPOL spectropolarimeter visitor instrument. Using the technique of least-squares deconvolution to increase the signal-to-noise ratio of the data, we have applied Zeeman Doppler imaging to reconstruct brightness and magnetic surface topologies of the star. The brightness image shows a large polar spot with weaker low- to mid-latitude features, confirming an earlier Doppler imaging observation. The reconstruction of the surface magnetic field shows regions of radial field at all latitudes (except near the pole) and regions of azimuthal field predominantly at high latitudes (60°–70°), with the azimuthal field almost forming a ring around the polar regions.

We have incorporated a solar-like differential rotation law into the imaging process to determine the surface differential rotation of cool spots on HD 171488. This gives an equatorial rotation rate of 1.313 ± 0.004 d and a surface shear of $\mathrm{d}\Omega = 0.402 \pm 0.044$ rad d^{-1}. This means that the equator of HD 171488 laps the poles every $\sim 16 \pm 2$ d and that HD 171488 has a photospheric shear approximately seven times the solar value. This is the largest measurement of surface differential rotation yet obtained using the Doppler imaging method and is over twice the value of previously observed early G-dwarfs.

Key words: line: profiles – stars: activity – stars: imaging – stars: individual: HD 171488 – stars: magnetic fields – stars: spots.

1 INTRODUCTION

On the Sun the observed surface differential rotation (in which the equator laps the poles every ∼115 d) has been shown to extend down to the base of the solar convection zone. In this region (called the tachocline), strong shears formed by the interaction of the radiative zone rotating as a solid body and the differentially rotating convective zone, converts poloidal to toroidal magnetic field, the 'Ω-effect'. Thus, differential rotation plays a key role in the solar dynamo process, which generates the large-scale magnetic fields of the Sun. However, for stars other than the Sun, the operation of the magnetic dynamo and the involvement of differential rotation, is still not well understood.

Surface differential rotation has been measured on a number of solar-type stars using various methods, with Donati & Collier Cameron (1997) showing the first measurement of the magnitude of differential rotation on a single rapidly rotating star by cross-correlation of Doppler images of AB Dor taken several days apart. As an advance on this technique Petit, Donati & Collier Cameron (2002) developed a method of incorporating a solar-like differential rotation law into the Doppler imaging process and using a χ^2-minimization technique to determine the differential rotation of a star. Barnes et al. (2005b) have taken results based on this technique and shown that there appears to be little relationship between rotation rate and differential rotation, backing up the earlier findings of Hall (1991) that $\mathrm{d}P/P$ is proportional to P. Barnes et al. (2005b) instead found that spectral class is the more dominant effect with strong shears on G-dwarfs down to almost no differential rotation on M-dwarfs. For more massive stars, Reiners & Schmitt (2003a,b) and more recently Reiners (2006) have used line profile analysis to show that for inactive F- and G-stars relative differential rotation is more common in slower rotators. This result, however, may be affected by the fact that their sensitivity to relative differential rotation decreases with an increase in the rotation rate of the star.

⋆E-mail: marsden@astro.phys.ethz.ch (SCM); donati@obs-mip.fr (J-FD); semel@obspm.fr (MS); petit@ast.obs-mip.fr (PP); carterb@usq.edu.au (BDC)

In addition, Collier Cameron & Donati (2002); Donati, Collier Cameron & Petit (2003b) and Marsden, Carter & Donati (2005a) have shown that the surface differential rotation of active stars undergoes temporal fluctuations. These are interpreted as the fluctuating magnetic field, produced by a variable stellar dynamo, having a feedback effect on the stellar convective zone through the action of Lorentz forces. Such observations of differential rotation offer one of the few windows into the operation of the stellar dynamo.

Another such window is provided through the study of the photospheric magnetic fields of active solar-type stars. Spatial information on these magnetic fields can be investigated using spectropolarimetric observations by means of Zeeman Doppler imaging (ZDI, Semel 1989; Donati & Brown 1997). For solar-type stars, ZDI has mainly been used to observe K-dwarfs and giant/subgiant stars (i.e. Donati & Collier Cameron 1997; Donati 1999; Donati et al. 2003a; Petit et al. 2004b) with deeper convective zones than the Sun. These observations have shown that many of the stars have large regions of azimuthal magnetic field near the stellar surface often in the form of arcs or rings around the rotational axis of the star. In solar dynamo models, the large-scale azimuthal component of the magnetic field should be confined to the interface layer between the radiative and convective zones of the star and not be located near the stellar surface. As such it has been suggested that observations of near-surface azimuthal field imply that the dynamo process in these stars is distributed throughout the stellar convective zone, or at least it is active much closer to the stellar surface than in the solar case, indicating that the dynamos of these stars differ significantly from the solar dynamo.

In this paper, we present spectropolarimetric observations of the early G-dwarf HD 171488 (V889 Hercules, RA $= 18^{\rm h}34^{\rm m}20^{\rm s}$, Dec. $= +18^{\circ}41'25''$ J2000.0, Wichmann, Schmitt & Hubrig 2003). This is the first early G-dwarf to be imaged using ZDI, thus expanding the range of solar-type stars studied with this technique. HD 171488 is a young, bright (30–50 Myr, $W_{\rm Li} = 231 \pm 7$ mÅ, and $V_{\rm max} = 7.34$ Strassmeier et al. 2003), apparently single star, with relatively rapid rotation, $v \sin i$ measurements ranging from 33 (Henry, Fekel & Hall 1995) to 45 km s^{-1} (Cutispoto et al. 2002). Thus, it is an excellent target for ZDI. In fact, HD 171488 has been previously observed using Doppler imaging by Strassmeier et al. (2003), with these observations showing HD 171488 possessing a polar spot with the possibility of lower latitude features. Our paper describes the determination of both the brightness and the magnetic topologies of HD 171488 using ZDI for data taken in 2004 September at the Anglo-Australian Telescope (AAT). In addition, a solar-like differential rotation law has been incorporated into the imaging process to determine the surface differential rotation of the cool spot features on HD 171488.

2 OBSERVATIONS AND DATA REDUCTION

Spectropolarimetric observations in both left- and right-hand circularly polarized light of HD 171488 were obtained at the AAT over a five-night period of 2004 September 24–28. The observations were obtained using the SEMPOL spectropolarimeter (Semel, Donati & Rees 1993) visitor instrument in conjunction with the University College London Echelle Spectrograph (UCLES). The SEMPOL spectropolarimeter involves a fibre feed from the Cassegrain focus of the AAT to UCLES, where the two polarization states (in this case left- and right-hand circular polarization) are outputted in two fibres to UCLES with both polarization states being recorded simultaneously on the detector. Further information on the operation of the SEMPOL spectropolarimeter can be found in Semel et al. (1993) and Donati et al. (1997, 2003a).

The detector used for the observations was the EEV2 CCD with 2048×4096 $13.5\,\mu{\rm m}^2$ pixels. As the EEV2 is larger than the unvignetted field of UCLES a smaller window format (2048×2746 pixels) was used to reduce readout time. Using the 31 g mm^{-1} grating 45 orders (#129 to #85) were observed, giving a full wavelength coverage from 4342 to 6736 Å. However, due to a shift in the spectrograph on the last two nights (27th and 28th) order #129 partly fell off the chip and was not extracted, thus the wavelength range was reduced to 4375–6736 Å. The resolution obtained was around 70 000 (i.e. $\sim$4.3 km s^{-1}).

Observations in circular polarization (Stokes V) consist of a sequence of four exposures. Between each exposure the quarter-wave plate of the SEMPOL polarimeter is rotated between $+45^{\circ}$ and -45°, thus the polarization in each output fibre is alternated between exposures resulting in the removal of spurious polarization signals from the telescope and polarimeter (at least to a first-order approximation). Using this set-up, seven Stokes V observations of HD 171488 were obtained. As each Stokes V observation consists of four exposures this means that 27 Stokes I (intensity) observations of HD 171488 were simultaneously obtained (one exposure was severely contaminated by scattered moonlight, which affects the Stokes I observations more than the Stokes V, and was thus removed). A log of the spectropolarimetric observations of HD 171488 taken at the AAT is given in Table 1. The rotational phase of the observations was determined from the following ephemeris:

$$\mathrm{JD} = 2453274.5945 + 1.31\phi, \qquad (1)$$

where JD is the Julian date of the observation and ϕ is the rotational phase.

All raw frames were reduced into wavelength-calibrated spectra using the Echelle Spectra Reduction: an Interactive Tool (ESpRIT) optimal extraction routines of Donati et al. (1997). As the Zeeman signatures in atomic lines are extremely small (typical relative amplitudes of 0.1 per cent or less), we have applied the technique of least-squares deconvolution (LSD, Donati et al. 1997) to the over 2500 photospheric spectral lines in each echelle spectrum in order to create a single high signal-to-noise ratio (S/N) profile for each observation. The line mask used for the LSD was a G2 line list created from the Kurucz atomic data base and ATLAS9 atmospheric models (Kurucz 1993). The peak S/N of the initial Stokes I observations ranged from 40 to 140 (depending on observing conditions) while the peak S/N for the Stokes V observations (using four exposures) was 60–260. LSD has been applied to both the Stokes V and I data

Table 1. Log of spectropolarimetric AAT observations of HD 171488. The first two columns give the UT date and time of the centre of the observations, while the third column gives the exposure time. The fourth column gives the rotational cycle of the observations with the ephemeris used to calculate the phase given in equation (1).

UT date	UT time	Exposure time (s)	Rotational cycle
2004 September 24	09:48:46	4×600	-1.296 to -1.278
2004 September 25	09:04:18	4×600	-0.556 to -0.538
2004 September 25	10:44:52	4×600	-0.503 to -0.485
2004 September 26	09:21:05	4×600	0.216 to 0.234
2004 September 26	11:01:05	4×600	0.269 to 0.287
2004 September 27	10:51:48	4×600	1.026 to 1.048
2004 September 28	09:28:18	4×600	1.747 to 1.765

resulting in S/N values of 1100–2800 for the Stokes I profiles and 1800–10 900 for the Stokes V profiles. This corresponds to an average multiplex gain of ∼18 for the Stokes I observations and ∼38 for the Stokes V observations. The multiplex gain for the Stokes I profiles is significantly less than that for the Stokes V profiles because, as pointed out by Donati et al. (1997), the technique of LSD appears to be not as suited to Stokes I as it is to Stokes V. The S/N of the LSD profiles has been calculated from measuring the noise in the wings of the profiles. Further information on LSD can be found in Donati et al. (1997).

In order to correct wavelength shifts of instrumental origin, each spectrum was shifted to match the Stokes I LSD profile of the telluric lines contained in the spectrum, as was done by Donati et al. (2003a). This reduces the relative radial velocity shifts of the LSD profiles to less than 0.1 km s^{-1}.

3 SURFACE IMAGES OF HD 171488

Surface images of rapidly rotating stars can be obtained through the inversion of a time-series of LSD profiles via the Doppler imaging technique. However, this inversion is an ill-posed problem with an infinite number of solutions that can be found to fit the data. To choose a unique solution some additional constraint, often called regularization, is usually applied, although there are other techniques such as the CLEAN-like Doppler imaging of Kürster (1993) and the Occamian method of Berdyugina (1998). An overview of some of the Doppler imaging methods available is given by Rice (2002). Two of the most common regularization schemes used are the Tichunov method which minimizes local gradients and produces the smoothest image, and the maximum-entropy method, first used by Vogt, Penrod & Hatzes (1987) which produces the image with the minimum amount of information required to produce the observed spectroscopic variations. However, as the data quality increases the role of the regularization scheme is reduced and image differences are minimized.

Our brightness and magnetic images of HD 171488 were created using the ZDI code of Brown et al. (1991) and Donati & Brown (1997), using the Stokes I and V LSD profiles as inputs for the brightness and magnetic mapping, respectively. This code implements the Skilling & Bryan (1984) maximum-entropy optimization scheme which, as mentioned, produces an image with the minimum amount information. The effect modelled stellar parameters have on images created using maximum-entropy optimization are discussed in a number of papers including that of Vogt et al. (1987) and more specifically for our code Donati & Brown (1997).

3.1 Fundamental parameters of HD 171488

In order to determine the parameters used in the reconstruction of the surface topologies of HD 171488 [namely $v \sin i$ and radial velocity; photospheric and spot temperatures were determined from the Doppler images of Strassmeier et al. (2003), see Section 3.2], the χ^2-minimization technique was used, see Barnes et al. (2000). In this method, the parameters that simply give the best fitting to the data (lowest reduced-χ^2 values) are chosen. This was done using the Stokes I data as there are more profiles, and the magnetic images were then reconstructed using the same values. The values used in the image reconstruction of HD 171488 are given in Table 2. These values are in reasonable agreement with those found by Strassmeier et al. (2003).

The other parameter required for Doppler/Zeeman Doppler imaging is the inclination angle of the star and it is often the most difficult parameter to determine. We have used the absolute bolometric magnitude of HD 171488 ($M_{\rm bol} = 4.42 \pm 0.07$; Strassmeier et al. 2003) which was determined from the maximum observed brightness of the star and the *Hipparcos* distance of 37.2 ± 1.2 pc. Given $T_{\rm eff\odot} = 5780$ K, $M_{\rm bol\odot} = 4.74$ and $\rm BC_V = -0.07$ (for a temperature of 5750 K) all taken from Bessell, Castelli & Plez (1998) and assuming a photospheric temperature for HD 171488 of 5800 ± 100 K (based on the maximum temperature in the Doppler images of Strassmeier et al. 2003) this implies that HD 171488 has a luminosity of 1.34 ± 0.09 $\rm L_\odot$ and a radius of 1.15 ± 0.08 $\rm R_\odot$ (Strassmeier et al. 2003 give 1.33 ± 0.09 $\rm L_\odot$ and 1.09 ± 0.05 $\rm R_\odot$). Given the equatorial period of 1.313 ± 0.004 d found in Section 3.4 and the $v \sin i$ of 37.5 ± 0.5 km s^{-1} (Table 2), this implies that the inclination angle of HD 171488 is $58 \pm 9^\circ$. This is likely to be a slight overestimate as the maximum brightness of the star is likely to be dimmer than the star's unspotted brightness. By way of comparison, the χ^2-minimization method gives an inclination angle of $\sim 65^\circ$. We have chosen to use 60° as the inclination angle of the star. This is slightly higher than the 55° used by Strassmeier et al. (2003). A limb-darkening coefficient of 0.66 has been assumed in the imaging process.

3.2 Brightness image

In order to reconstruct the brightness image of HD 171488, the imaging code uses a two-temperature model (one for cool spots and one for the quiet photosphere, as described by Collier Cameron 1992), where for each image pixel the local relative area occupied by cool spots (spot occupancy) is reconstructed.

As has been done by Petit et al. (2002, 2004b) and Marsden et al. (2005b), we have used synthetic Gaussian profiles to represent the

Table 2. Fundamental parameters of HD 171488 used in this paper. The photospheric and spot temperatures have been taken from the Doppler images of Strassmeier et al. (2003); see Section 3.2, while the equatorial rotational period has been determined from the surface differential rotation, see Section 3.4. Also listed are the values given by Strassmeier et al. (2003).

Parameter	Our value	Strassmeier et al.'s value
Photospheric temperature	5800 K	5830 ± 50 K
Spot temperature	4200 K	
Radius	1.15 ± 0.08 $\rm R_\odot$	1.09 ± 0.05 $\rm R_\odot$
$v \sin i$	37.5 ± 0.5 km s^{-1}	39.0 ± 0.5 km s^{-1}
Radial velocity ($v_{\rm rad}$)	-22.7 ± 0.3 km s^{-1}	-23.6 ± 1.5 km s^{-1}
Inclination angle (i)	$60^\circ \pm 10^\circ$	$\sim 55^\circ$
Equatorial rotational velocity ($v_{\rm eq}$)	44 ± 3 km s^{-1}	
Equatorial rotation period ($P_{\rm eq}$)	1.313 ± 0.004 d	1.3371 ± 0.0002 d

profiles of both the spot and the photosphere. It has been shown by Unruh & Collier Cameron (1995) that there is little change in the spot maps when using synthetic profiles over profiles created from slowly rotating comparison stars. Synthetic profiles were chosen, as the imaging code tends to converge more smoothly. We have used the same Gaussian profile to represent both the spot and the photosphere, as was done for the early G-dwarf R58 (Marsden et al. 2005b). The full width at half-maximum (FWHM) of the Gaussian was set to 9 km s^{-1} matching the FWHM of the Moon's LSD profile (taken with the same instrumental set-up). The temperature of the spots and the quiet photosphere were taken from the maximum and minimum temperatures of the average map of HD 171488 (see Strassmeier et al. 2003, fig. 7a). These corresponded to ∼5800 K for the photosphere and ∼4200 K for the spot. Thus, the photosphere-spot temperature difference is ∼1600 K. This value is slightly below the photosphere-spot contrast graph of Berdyugina (2005), which indicates a temperature difference of ∼1800–1900 K for a photospheric temperature of 5800 K.

During the last two nights of observations (27th and 28th), there was some cloud present. This had the effect of not only reducing the amount of signal received but also scattering Moonlight into the spectrograph. This led to a small 'dip' in the centre of the LSD profile, similar to that seen in observations of R58 (see Marsden et al. 2005b, fig. 5). A similar method to that used by Marsden et al. (2005b) was used here to remove the solar contamination in the LSD profiles, by scaling and subtracting an LSD profile of the Moon taken with the same instrumental set-up around the same time as the observations. However, as the profiles around phase 0.0 are all contaminated and there are no other profiles nearby in phase with which to determine the 'uncontaminated' profile this means that the solar contamination removed from these profiles is likely to be an underestimate. Due to this, there is possibly a slight misfit to the data for those profiles around phase 0.0 which could result in some spots not being recovered around this phase. Other minor misfits to the LSD profiles are likely to be the result of noise in the profiles. The solar contamination only affects the Stokes I profiles, so no adjustment was required for the Stokes V profiles.

The maximum-entropy brightness image reconstruction for HD 171488 is shown in Fig. 1 (top left-hand image) created fitting the data down to the noise level and has a spot filling factor of ∼0.055 (meaning spot covers ∼5.5 per cent of the total stellar surface). Fits of the modelled profiles to the observed LSD profiles are given in Fig. 2.

The brightness image of HD 171488 (Fig. 1, top left-hand image) shows a large polar spot extending down to almost +60° latitude. This agrees with the Doppler image of Strassmeier et al. (2003), although our polar spot would appear to extend to lower latitudes than theirs. This increase in the size of the polar spot may be due to the slightly larger inclination angle, we have used in the imaging process over that of Strassmeier (see Section 3.1). It has been previously shown by Marsden et al. (2005b) that an increase in the modelled inclination angle leads to an increase in the intensity of the mid- to high-latitude features. However, the overall spot structure appears to be maintained through changes in the modelled inclination angle. Strassmeier et al. (2003) also reported the possibility of low- to mid-latitude features; however, they concluded that they were too weak to be judged significant. With the excellent S/N of our data (1000+), we can confirm the presence of such features with two relatively intense spots at a latitude of ∼+30° and phases of 0.75 and 0.85. Other lower latitude features are also present but are of lesser

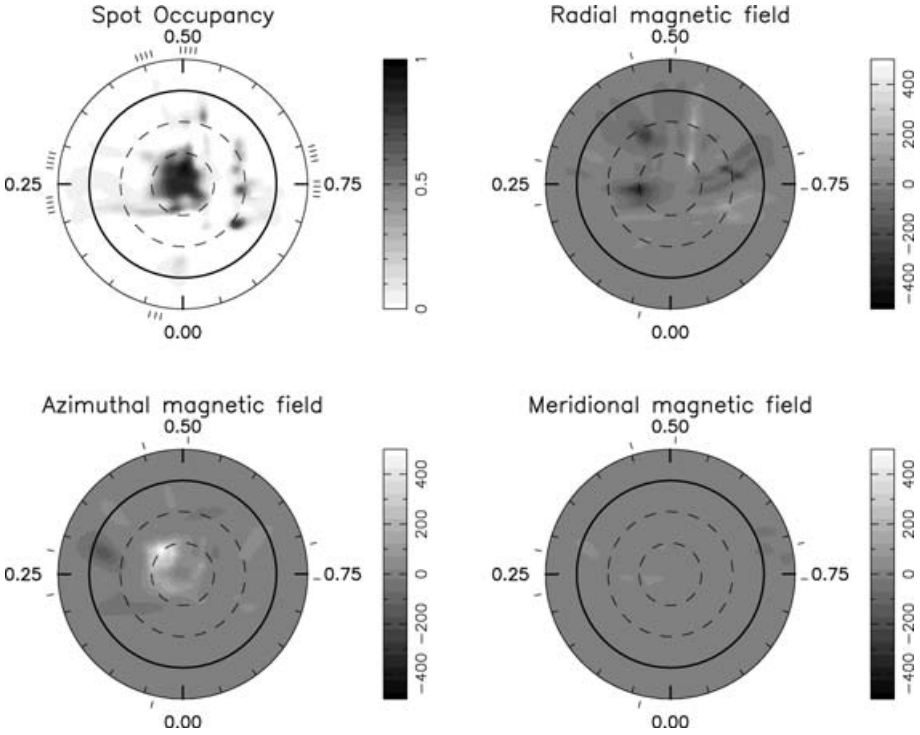

Figure 1. Maximum-entropy brightness and magnetic image reconstructions for HD 171488, 2004 September 24–28. The images are flattened polar projections extending down to −30° latitude. The bold lines denote the equator and the dashed lines are +30° and +60° latitude parallels. The radial ticks outside the plots indicate the phases at which the star was observed. The scale in the magnetic images is in gauss. The brightness image (top left-hand image) has a spot filling factor of ∼0.055 (or 5.5 per cent), while the magnetic images have a mean field modulus of 31 G. The images have been created with the inclusion of the surface differential rotation of the star, see Section 3.4.

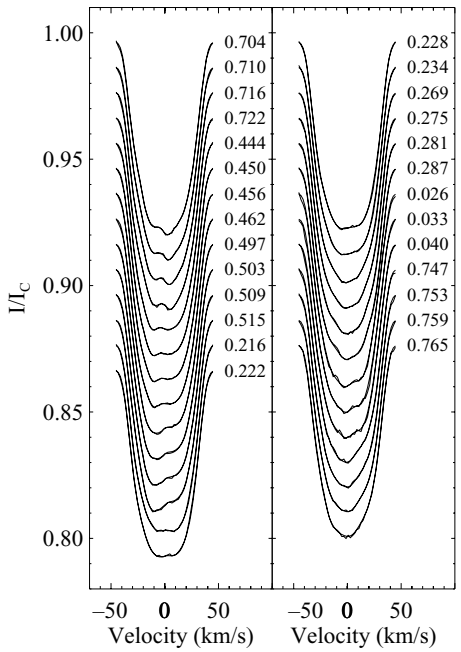

Figure 2. Maximum-entropy fits for the Stokes I LSD profiles of HD 171488, 2004 September 24–28. The thin lines represent the observed LSD profiles while the thick lines represent the fits to the profiles produced by the imaging code. Each profile is shifted down by 0.01 for graphical purposes. The rotational phases at which the observations took place are indicated to the right of each profile.

intensities. The inclination angle of the star means that there should be little or no north–south mirroring in the reconstructed image (i.e. spots in the *Southern* hemisphere of the star should not be mapped on to the *Northern* hemisphere). Due to the effect of limb darkening, spot features in the *Southern* hemisphere of the star are usually very faint and thus as expected there are virtually no features recovered below the stellar equator.

The variation in spot occupancy with stellar latitude is given in Fig. 3, which plots fractional spottedness versus stellar latitude. Fractional spottedness is defined as

$$F(l) = \frac{S(l)\cos(l)\,\mathrm{d}l}{2}, \qquad (2)$$

where $F(l)$ is the fractional spottedness at latitude l, $S(l)$ is the average spot occupancy at latitude l, and dl is the latitude width of each latitude ring.

3.3 Magnetic images

For HD 171488, we have reconstructed the magnetic field topology using ZDI. Using Stokes V spectropolarimetric data, the ZDI code can reconstruct images of radial, azimuthal, and/or meridional fields, or any combination of these. ZDI measures mainly large-scale magnetic fields, flux that is contained in small dipoles below the resolution limit of the observations (in this case $\sim$10° in longitude at the stellar equator) is not recovered. The reconstructed magnetic fields are shown in Fig. 1. The fits to the Stokes V LSD profiles are given in Fig. 4. The images were again created fitting the data to the noise level and resulted in a mean field modulus of 31 G.

As noted in Section 3.2, the observations on the last two nights (the 27th and 28th) were affected by cloud. This means that the S/Ns of the Stokes profiles are significantly reduced. This is especially

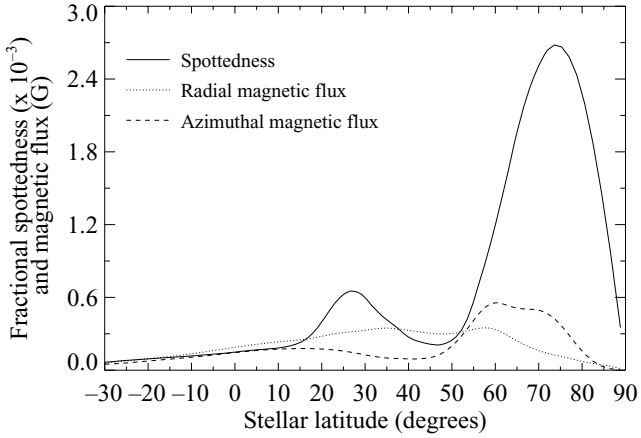

Figure 3. Fractional spottedness and magnetic flux versus stellar latitude for HD 171488. Fractional spottedness/magnetic flux is based on the average spot occupancy/absolute value of the magnetic field at each latitude and is defined by equation (2).

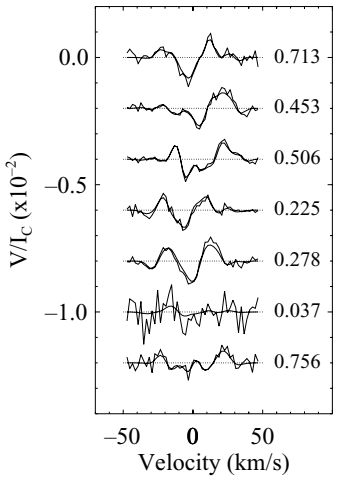

Figure 4. Maximum-entropy fits for the Stokes V LSD profiles of HD 171488, 2004 September 24–28. The thin lines represent the observed LSD profiles while the thick lines represent the fits to the profiles produced by the imaging code. Each profile is shifted down by 0.002 for graphical purposes. The rotational phases at which the observations took place are indicated to the right of each profile.

true of the observation on the night of the 27th at around phase 0.0, where there was no detection of a magnetic field in the Stokes V profile (see profile second from bottom in Fig. 4). This means that there is little or no constraint on the magnetic image around this phase. As discussed by Donati (1999), ZDI is mostly sensitive to radial/meridional field features located close to the phase of observations and to azimuthal field located about 0.2 phase away from the phase of observations. Therefore, it is not surprising that little or no radial field is reconstructed around phase 0.0 (see top right-hand image in Fig. 1) for HD 171488.

When using circular polarimetry alone (Stokes V) all three field components (radial, azimuthal and meridional) can be recovered for high-latitude features, however, for low-latitude features ZDI suffers some cross-talk between radial and meridional field components (Donati & Brown 1997). This is especially true for stars with low stellar inclinations, but for HD 171488 with an inclination of $i \sim 60°$ this should be minimized. In addition, the sensitivity of ZDI to

low-latitude meridional fields decreases significantly with an increase in stellar inclination angle. For high-inclination stars, such as the young K-dwarf AB Dor and HD 171488 (both $i \sim 60^\circ$), the ZDI code is very insensitive to low-latitude meridional field, but this is not true for high latitude meridional fields. As the lower right-hand image in Fig. 1 shows there is virtually no meridional field seen on HD 171488. This implies that such field is not present or very weak at high latitudes on HD 171488, similar to that seen on AB Dor.

Fig. 1 also shows that there is virtually no magnetic field (of any type) reconstructed at the stellar pole. Again, this is typical of stars with polar spots and is believed to be due to the reduced flux from the dark polar spot and the fact that molecular lines start to dominate over atomic lines (which ZDI uses) within the lower temperatures of the polar spot.

The fractional magnetic flux versus stellar latitude for both the radial and azimuthal magnetic field have been plotted in Fig. 3. Fractional magnetic flux has been calculated the same way as fractional spottedness from equation (2) using the absolute value of the magnetic field.

3.4 Surface differential rotation

In order to measure the surface differential rotation of HD 171488, a simplified solar-like differential rotation law was incorporated into the imaging process:

$$\Omega(l) = \Omega_{\rm eq} - {\rm d}\Omega \sin^2 l \ ({\rm rad\ d^{-1}}), \tag{3}$$

where $\Omega(l)$ is the rotation rate at latitude l, $\Omega_{\rm eq}$ is the equatorial rotation rate and dΩ is the rotational shear between the equator and the poles. The surface differential rotation can then be determined by treating both $\Omega_{\rm eq}$ and dΩ as free parameters and determining the best fitting to the data using the χ^2-minimization method of Petit et al. (2002). This was done for both the brightness and magnetic data; however, a measurement could only be determined from the brightness data as the magnetic data did not give out the paraboloid shape discussed below. This is probably due to the limited number of Stokes V observations.

For the brightness data, the imaging code was forced to converge to a fixed spot filling factor of 0.055 (the level of spot coverage on the reconstructed image, see Fig. 1, determined iteratively) for various values of $\Omega_{\rm eq}$ and dΩ producing a level of fit for each pair of values. This created the reduced-χ^2 landscape shown in Fig. 5. It should be noted that the minimum-χ^2 value does not quite reach 1.0. As discussed in Barnes et al. (2005a), this has no effect on the results as it is the change in χ^2 from the minimum value that is important. Fitting a paraboloid to the data in Fig. 5 gives $\Omega_{\rm eq} = 4.786 \pm 0.013$ rad d^{-1} and ${\rm d}\Omega = 0.402 \pm 0.044$ rad d^{-1}, with the errors being 1σ errors. The value of $\Omega_{\rm eq}$ is equivalent to an equatorial rotation period of 1.313 ± 0.004 d while the dΩ value corresponds to $\sim 16 \pm 2$ d for the equator to lap the poles. This is the largest value of dΩ yet measured using this method. The fit assuming solid body rotation is over 10σ higher than that for the differential rotation values given above, indicating a definite detection of surface differential rotation. Further examination of this result is carried out in Section 4.2.

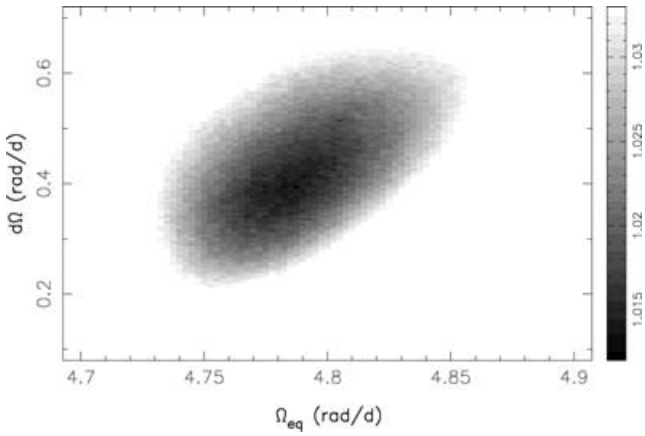

Figure 5. Surface differential rotation χ^2 minimization for HD171448, 2004 September 24–28. The image shows the reduced-χ^2 values obtained from the maximum-entropy imaging code for various values of $\Omega_{\rm eq}$ and dΩ given a fixed spot coverage of 0.055 and an inclination angle of 60°. Darker regions correspond to lower reduced-χ^2 values. The grey-scale image projects $\pm 5\sigma$ on to the axes in both $\Omega_{\rm eq}$ and dΩ.

4 DISCUSSION

4.1 Magnetic topology

Fig. 1 (top right-hand image) shows that the radial magnetic field of HD 171488 has no real latitude dependence with both positive and negative field at almost all latitudes, except near the pole. Although the negative field would appear to dominate over the positive, this could well be an effect of the poor observation at phase 0.0 (see Section 3.3). The fractional radial magnetic flux in Fig. 3 shows that (other than the lack of features at the pole), there appears to be no preferential latitude for the distribution of the radial magnetic field. This appears to be fairly typical for active solar-type stars observed using ZDI, for example, the lower mass K-stars such as AB Dor and LQ Hya, (Donati et al. 2003a) and the higher mass F-star HR 1817 (Mengel 2006).

The azimuthal field, however, does appear to show a strong latitude dependence. Fig. 1 (bottom left-hand image) shows that HD 171488 has a region of positive azimuthal field at around 60° latitude. This almost forms a ring around the stellar rotational axis. Such latitude dependence of the azimuthal magnetic field has been observed on other stars, with rings of azimuthal field being observed previously on the giant/subgiant stars HR 1099 and HD 199178 (i.e. Donati et al. 1992, 2003a; Petit et al. 2004a,b), the K-dwarf AB Dor (Donati et al. 2003a), and the late F-dwarf HR 1817 (Mengel 2006). Such near-surface regions of azimuthal field have been cited by Donati et al. (2003a) and Petit et al. (2004b), among other references, as evidence for the stellar magnetic dynamo of these stars being distributed throughout the stellar convective zone, rather than restricted to the tachocline, as in the solar case.

The formation of high-latitude rings of azimuthal field in active stars is an indication of the dynamo mechanism in operation in these stars. Further observations of solar-type stars, such as HD 171488, may shed more light on this phenomenon.

The ring of azimuthal field on HD 171488 lies just outside the peak of the fractional spottedness as shown in Fig. 3. The fact that the areas of azimuthal field often lie just outside the polar spot has been mentioned by Donati et al. (1992) and Solanki (2002) as possibly due to the twisting of the Evershed flow in the penumbra of the polar spot. This twisting is either due to the Coriolis force and/or strong polar differential rotation. While this may be able to explain the production of rings of azimuthal field outside the polar spot, is is unlikely to be correct for two reasons. The first is that this assumes that the magnetic field in the polar spot is unipolar. This

appears to be untrue as polar spots are believed to contain regions of differing polarity, as discussed by Jardine et al. (2002). This has also been seen in the Zeeman Doppler images of other stars with mixed polarity fields at high latitudes (Donati et al. 2003a). Secondly it does not account for the banding (and more complex structures) of azimuthal field seen in some ZDI images (e.g. Donati et al. 2003a, Fig. 23).

Donati et al. (2003a) showed that for the young K-dwarfs AB Dor and LQ Hya, magnetic energy concentrates preferentially in the toroidal field rather than the poloidal field, with the azimuthal field component containing ∼60 per cent of the total magnetic energy (∼40 per cent radial) at most observing epochs. If we ignore the contribution from meridional field (small on our maps) then for HD 171488 the azimuthal field component is slightly more dominant than the radial with ∼55 per cent of the quadratic field energy. This value may be affected by the lack of constraint on the magnetic images at around phase 0.0. Given that it is the radial field that is likely to be missing from the images (as ZDI is mostly sensitive to radial field around the phase of the observations, but to azimuthal field about 0.2 phase from the phase of the observations), then it is possible that the radial and magnetic field may be more evenly balanced. However, data with moderate phase coverage are more prone to cross-talk between field components and thus the ratio of azimuthal and radial field should only be taken as an indication at the moment.

The average intensity of the field on HD 171488 (∼30 G) is significantly lower that of lower mass solar-type stars (AB Dor ∼125 G and LQ Hya 50–100 G, Donati et al. 2003a). Again, this could be slightly influenced by the lack of phase coverage on the star. Rotation rate also plays a part as the resolution element is larger for slower rotators (assuming a similar observational resolution). While this may account for the smaller value for HD 171488 when compared to AB Dor, it does not when HD 171488 is compared to LQ Hya (AB Dor $v \sin i = 89$ km s^{-1} and LQ Hya $v \sin i = 26$ km s^{-1}, both have $i = 60^\circ$, Donati et al. 2003a). It is thus not unreasonable to conclude that the thinner convective zone of HD 171488 is responsible for the reduced magnetic field strength observed on HD 171488.

4.2 Surface differential rotation

The level of surface differential rotation we have determined for HD 171488 is the strongest photospheric shear that has yet been measured using the Doppler imaging method, although the error bars are somewhat large due to the limited amount of observations. Barnes et al. (2005b) have recently published results showing the dependence of surface differential rotation on spectral class. This shows an increase from almost solid body rotation for M-dwarfs up to surface differential rotation rates around three times the solar value for early G-dwarfs. For HD 171488, we find a level of surface differential rotation around seven times that of the solar value, over twice that observed on the two early G-dwarfs previously observed (see Table 3). Petit et al. (2002) discussed that data with limited phase coverage (as we have here) can produce an inflated value for dΩ, with an increase of ∼30 per cent when cutting the number of observations in half. However, this increase is not enough to account for the high level of dΩ that we find for HD 171488. Petit et al. (2002) also stated that for small errors in the modelled $v \sin i$ value (of the order of 1–2 per cent as we have here, see Table 2), there is almost no impact on the measured surface differential rotation.

As mentioned in Section 3.1, inclination angle is often the hardest parameter to determine. Marsden et al. (2005b) have shown that an error of $\pm 10^\circ$ in the inclination angle, as we have estimated in Table 2, can have an effect on the measured surface differential rotation. In order to test what effect the modelled inclination angle could have here, we have determined the surface differential rotation for HD 171488 using inclination angles of 50° and 70° (in addition to the $i = 60^\circ$ results given in Section 3.4). The measured surface differential rotation for both $i = 50^\circ$ and 70° were found to be within the error bars of the $i = 60^\circ$ result. Thus, an incorrectly modelled inclination angle appears not to be responsible for the high level of differential rotation we observe on HD 171488.

It is possible that during the five nights of observations, a new spot emerged on the surface of HD 171488 throwing off the surface differential rotation measurement, although this is unlikely in the time-frame of ∼4 d (approximately three rotations). Previous experience of young solar-type stars has shown that spot features are usually broadly stable on time-frames of approximately a week, although Wolter, Schmitt & van Wyk (2005) claimed significant spot evolution on the ultrarapid rotator 'Speedy-Mic' in as little as 5 d (corresponding to about 13 rotations). If a new spot did emerge, this is most likely to have happened near phase 0.75 where there are overlapping observations and where Fig. 1 (top left-hand image) shows two similarly sized spots at around $+30^\circ$ latitude. We have attempted to recreate the brightness image of HD 171488 assuming no surface differential rotation and both spots are still reproduced. Even removing the last night of observations (the 28th at around phase 0.75) still produces two distinct spot features. We therefore think that the emergence of a new spot is an unlikely explanation for HD 171488's high level of surface differential rotation.

Table 3. Comparison of the stellar parameters of the three early G-dwarfs that have had their surface differential rotation measured using Doppler imaging. Except where noted, the data for HD 171488 come from Strassmeier et al. (2003), while the data for R58 come from Marsden et al. (2005a,b) and the data for LQ Lup come from Donati et al. (2000).

Parameter	HD 171488	R58	LQ Lup
$(B-V)$	0.62[a]	0.61[b]	0.69[c]
Age	30–50 Myr	35 ± 5 Myr	25 ± 10 Myr
Mass	1.06 ± 0.02 M$_\odot$	1.15 ± 0.05 M$_\odot$	1.16 ± 0.04 M$_\odot$
Radius	1.15 ± 0.08 R$^d_\odot$	$1.18^{+0.17}_{-0.10}$ R$_\odot$	1.22 ± 0.12 R$_\odot$
$\Omega_{\rm eq}$	4.786 ± 0.013 rad d^{-1}[e]	11.139 ± 0.008 rad d^{-1} (2000 January) 11.190 ± 0.006 rad d^{-1} (2003 March)	20.28 ± 0.01 rad d^{-1}
dΩ	0.402 ± 0.044 rad d^{-1}[e]	0.025 ± 0.015 rad d^{-1} (2000 January) 0.138 ± 0.011 rad d^{-1} (2003 March)	0.12 ± 0.02 rad d^{-1}

[a]From Cutispoto et al. (2002); [b]from Randich (2001), dereddened value; [c]from Wichmann et al. (1997); [d]from this paper, Strassmeier et al. (2003) give 1.09 ± 0.05 R$_\odot$; [e]from this paper.

There are only two other early G-dwarfs that have had their surface differential rotation measured using Doppler imaging, these are R58 (HD 307938, Marsden et al. 2005a,b) and LQ Lup (Donati et al. 2000). LQ Lup has only been observed once giving a photospheric shear of $d\Omega = 0.12 \pm 0.02$ rad d^{-1}, while R58 has been observed twice and gives a large range of shear values, in 2000 $d\Omega = 0.025 \pm 0.015$ rad d^{-1} and in 2003 $d\Omega = 0.138 \pm 0.011$ rad d^{-1}. Reiners (2006) has also observed R58 and, using line profile analysis, found no evidence of differential rotation. The stellar parameters of the three stars are given in Table 3. HD 171488 has a $d\Omega$ value over twice that of both these stars (even accounting for the large error in the HD 171488 measurement). The ages, masses and radii of R58 and LQ Lup are not too dissimilar to that of HD 171488, therefore the evolutionary state of HD 171488 offers no indication of a reason for such a high surface differential rotation. Also the slower rotation of HD 171488 compared to that of LQ Lup and R58 should not be responsible as Barnes et al. (2005b) showed only slight (if any) dependence of surface differential rotation on rotation rate and show a slight decrease in $d\Omega$ with an increase in rotational period.

Recently a star with an even higher mass than HD 171448 has been observed by Mengel (2006), the late F-dwarf HR 1817. The surface differential rotation for HR 1817 was measured using the same method we have used here but using magnetic (Stokes V) rather than spot (Stokes I) features. These results showed that HR 1817 has a $d\Omega = 0.256 \pm 0.017$ rad d^{-1}. While this is higher than that predicted by the power law of Barnes et al. (2005b) for a late F-star, it is significantly below that of HD 171488. Donati et al. (2003b) showed differences in differential rotation measurements from magnetic and spot features and suggested that they are anchored at different depths in the convective zone, thus implying a change in the convective zone differential rotation with depth. Such a comparison of magnetic and brightness differential rotation rates has currently only been done for K-dwarfs and shows that differential rotation measured from brightness (Stokes I) profiles appears to be consistently lower than that measured from magnetic (Stokes V). It is still unknown whether this is true for stars with thinner convective zones.

What the high differential rotation rates for HD 171488 and HR 1817 do show is that differential rotation appears to increase significantly as convective zone depth decreases. A finding supported by the theoretical models of Kitchatinov & Rüdiger (1999) and more recently by Küker & Rüdiger (2005) which show an increase in differential rotation with decreasing convective zone depth due to a shorter convective turnover time-scale. Although the increase in differential rotation predicted by theory is not as significant as that measured from observations. A rapid increase in differential rotation with decreasing convective zone depth is also supported by the recent work of Reiners (2006), where the differential rotation of a number of mostly F-stars has been determined by line profile analysis. These results show a number of stars with $d\Omega\sqrt{\sin(i)}$ (called absolute shear by Reiners) in excess of 0.5 rad d^{-1}, although only about 20 per cent of the stars showed evidence of non-solid-body rotation. Thus, it could be that HD 171488 is 'bridging the gap' between the mostly strong differential rotation measurements found on F-stars using line profile analysis and the usually weaker differential rotation measurements (from G-, K- and M-stars) found using the Doppler imaging technique. However, this still does not account for why HD 171488 shows such high differential rotation with respect to other early G-dwarfs measured using the same technique.

The large temporal change in $d\Omega$ of R58 (see Table 3) may indicate that G-dwarfs undergo significant temporal variations in surface differential rotation similar to the variations evidenced on K-dwarfs (Donati et al. 2003b), but on a larger scale. If this is so, then perhaps we have observed HD 171488 near the peak of its surface differential rotation. Once again, further observations of HD 171488 (and other higher mass solar-type stars) may help to clarify this issue.

Finally, Table 2 shows a significant difference between the rotational period we calculate and that of Strassmeier et al. (2003) that cannot be accounted for by the errors in the measurements. This difference is due to the differential rotation of the star. While our value is the equatorial rotation period of the star, the Strassmeier et al. (2003) value is based on star-spot photometry and is dependent upon the latitude of the star-spots observed. Using equation (3), the value of $d\Omega$ for HD 171488 of 0.402 ± 0.044 rad d^{-1}, and the equatorial rotational period of 1.313 ± 0.004 d, this implies that the polar rotation rate of HD 171488 is 1.43 ± 0.02 d. Thus, the photometric period of Strassmeier et al. (2003) falls between the equatorial and polar rotation rates of HD 171488 and in fact, corresponds to a latitude of $\sim 30^\circ$.

5 CONCLUSIONS

In this paper, we have presented reconstructed brightness and magnetic images of the young solar-type star HD 171488. The brightness image has shown that HD 171488, like many rapidly rotating solar-type stars possesses a reasonably large polar spot with less intense low- and mid-latitude features. The magnetic images have revealed regions of azimuthal field near the stellar surface, which along with similar fields reported for other rapid rotators suggests that the dynamo mechanism in such stars may lie close to the stellar surface. In addition, the make-up of the magnetic field structure (i.e. the ratio of azimuthal and radial field) as well as the overall strength of the magnetic field may well be different to that of lower mass solar-type stars. We have also shown that HD 171488 possesses the strongest surface differential rotation rate measured using the Doppler imaging method, with a surface shear approximately seven times the solar value. The reasons why HD 171488 should have such a strong differential rotation are currently unclear, although it appears to support the findings of strong shear on F-stars by Reiners (2006).

The effect of decreasing convective zone depth on the operation of the stellar dynamo and the role of differential rotation are still not well understood. However, it would appear that convective zone depth is the dominant factor in the level of surface differential rotation exhibited by a star. Whether or not this differential rotation is continued down to the base of the convective zone, as in the Sun, is not known. Our current limited understanding of the operation of the stellar magnetic dynamo, especially in thinner convective envelopes, is hindered by a lack of available data. Thus, we encourage more observations (and in particular spectropolarimetric observations) of higher mass solar-type stars to help improve this situation.

ACKNOWLEDGMENTS

We would like to thank the anonymous referee for his assistance in improving this paper. The observations in this paper were obtained with the AAT. We would also like to thank the technical staff of the Anglo-Australian Observatory for their excellent assistance during these observations. This work was partly supported by ETH Research Grant TH-3/05-1.

REFERENCES

Barnes J. R., Collier Cameron A., James D. J., Donati J.-F., 2000, MNRAS, 314, 162

Barnes J. R., Collier Cameron A., Lister T. A., Pointer G. R., Still M. D., 2005a, MNRAS, 356, 1501

Barnes J. R., Collier Cameron A., Donati J.-F., James D. J., Marsden S. C., Petit. P., 2005b, MNRAS, 357, L1

Berdyugina S. V., 1998, A&A, 338, 97

Berdyugina S. V., 2005, Starspots: A Key to the Stellar Dynamo, Living Rev. Solar Phys. 2, (2005), 8. URL (cited on 2005 December 13): http://www.livingreviews.org/lrsp-2005-8

Bessell M. S., Castelli F., Plez B., 1998, A&A, 333, 231

Brown S. F., Donati J.-F., Rees D. E., Semel M., 1991, A&A, 250, 463

Collier Cameron A., 1992, in Byrne P. B., Mullan D. J., eds, Lecture Notes in Physics, Vol. 397, Surface Inhomogeneities on Late-Type Stars. Springer, Berlin, p. 33

Collier Cameron A., Donati J.-F., 2002, MNRAS, 329, L23

Cutispoto G., Pastori L., Pasquini L., de Medeiros J. R., Tagliaferri G., Andersen J., 2002, A&A, 384, 491

Donati J.-F., 1999, MNRAS, 302, 457

Donati J.-F., Brown S. F., 1997, A&A, 326, 1135

Donati J.-F., Collier Cameron A., 1997, MNRAS, 291, 1

Donati J.-F., Brown S. F., Semel M., Rees D. E., Dempsey R. C., Matthews J. M., Henry G. W., Hall D. S., 1992, A&A, 265, 682

Donati J.-F., Semel M., Carter B. D., Rees D. E., Cameron A. C., 1997, MNRAS, 291, 658

Donati J.-F., Mengel M., Carter B. D., Marsden S., Collier Cameron A., Wichmann R., 2000, MNRAS, 316, 699

Donati J.-F. et al., 2003a, MNRAS, 345, 1145

Donati J.-F., Collier Cameron A., Petit P., 2003b, MNRAS, 345, 1187

Hall D. S., 1991, in Touminen I., Moss D., Rüdiger G., eds, Proceedings of Colloquium No. 130 of the International Astronomical Union, Vol. 380, The Sun and Cool Stars. Activity, Magnetism, Dynamos. Springer-Verlag, Berlin, Germany, p. 353

Henry G. W., Fekel F. C., Hall D. S., 1995, AJ, 110, 2926

Jardine M., Wood K., Collier Cameron A., Donati J.-F., Mackay D. H., 2002, MNRAS, 336, 1364

Kitchatinov L. L., Rüdiger G., 1999, A&A, 344, 911

Küker M., Rüdiger G., 2005, A&A, 433, 1023

Küster M., 1993, A&A, 274, 851

Kurucz R. L., 1993, CDROM #13 (ATLAS9 atmospheric models) and CDROM #18 (ATLAS9 and SYNTHE routines, spectral line database)

Marsden S. C., Carter B. D., Donati J.-F., 2005a, in Favata F., Hussain G. A. J., Battrick B., eds, Proceedings of the The 13th Cambridge Workshop on Cool Stars, Stellar Systems, and the Sun, ESA Special Publications, Vol. 560. ESA, Noordwijk, The Netherlands, P. 799

Marsden S. C., Waite I. A., Carter B. D., Donati J.-F., 2005b, MNRAS, 359, 711

Mengel M., 2006, Mphil thesis, University of Southern Queensland, Toowoomba, Queensland, Australia

Petit P., Donati J.-F., Collier Cameron A., 2002, MNRAS, 334, 374

Petit P. et al., 2004a, MNRAS 348, 1175

Petit P. et al., 2004b, MNRAS 351, 826

Randich S., 2001, A&A, 377, 512

Reiners A., 2006, A&A, 446, 267

Reiners A., Schmitt J. H. M. M., 2003a, A&A, 398, 647

Reiners A., Schmitt J. H. M. M., 2003b, A&A, 412, 813

Rice J. B., 2002, Astron. Nachr., 323, 220

Semel M., 1989, A&A, 225, 456

Semel M., Donati J.-F., Rees D. E., 1993, A&A, 278, 231

Skilling J., Bryan R. K., 1984, MNRAS, 211, 111

Solanki S. K., 2002, Astron. Nachr., 323, 165

Strassmeier K. G., Pichler T., Weber M., Granzer T., 2003, A&A, 411, 595

Unruh Y. C., Collier Cameron A., 1995, MNRAS, 273, 1

Vogt S. S., Penrod G. D., Hatzes A. P., 1987, ApJ, 321, 496

Wichmann R., Krautter J., Covino E., Alcalá J. M., Neuhäuser R., Schmitt J. H. M. M., 1997, A&A, 320, 185

Wichmann R., Schmitt J. H. M. M., Hubrig S., 2003, A&A, 399, 983

Wolter U., Schmitt J. H. M. M., van Wyk F., 2005, A&A, 435, 261

This paper has been typeset from a TEX/LATEX file prepared by the author.